UNCLASSIFIED

AD 273 060

Reproduced
by the

ARMED SERVICES TECHNICAL INFORMATION AGENCY
ARLINGTON HALL STATION
ARLINGTON 12, VIRGINIA

THE ORIGINAL PRINTING OF THIS DOCUMENT CONTAINED COLOR WHICH ASTIA CAN ONLY REPRODUCE IN BLACK AND WHITE

UNCLASSIFIED

NOTICE: When government or other drawings, specifications or other data are used for any purpose other than in connection with a definitely related government procurement operation, the U. S. Government thereby incurs no responsibility, nor any obligation whatsoever; and the fact that the Government may have formulated, furnished, or in any way supplied the said drawings, specifications, or other data is not to be regarded by implication or otherwise as in any manner licensing the holder or any other person or corporation, or conveying any rights or permission to manufacture, use or sell any patented invention that may in any way be related thereto.

62-2-5

273 060

ORIGINAL CONTAINS COLOR PLATES: ALL ASTIA REPRODUCTIONS WILL BE IN BLACK AND WHITE. ORIGINAL MAY BE SEEN IN ASTIA HEADQUARTERS.

Beckman & Whitley

SAN CARLOS, CALIFORNIA

ASTIA
RECEIVED
TISIA D

Beckman & Whitley INC.
SAN CARLOS, CALIFORNIA

ORIGINAL CONTAINS COLOR PLATES: ALL ASTIA REPRODUCTIONS WILL BE IN BLACK AND WHITE. ORIGINAL MAY BE SEEN IN ASTIA HEADQUARTERS.

PHENOMENA OF PENETRATION IN LIGHT WEIGHT RIGID PERSONNEL ARMOR MATERIALS

Final Report (Part A)

Dept. of Army
Quartermasters Research and
Engineering Command

Contract DA-19-129-QM-1574

Beckman & Whitley, Inc.
Research & Development Division

By:
J. W. Corcoran
J. M. Kelly

December 12, 1961

RD 63

AD _____ Accession No. _____

Beckman & Whitley, Inc., San Carlos, Calif.
PHENOMENA OF PENETRATION IN LIGHT WEIGHT PERSONNEL ARMOR MATERIALS - J. W. Corcoran and J. M. Kelly

Final Report, 12 Dec. 61, 59 pp., 16 illus., 5 tables.
(Contract DA-19-129-QM-1574) Proj. 7-80-05-001
Unclassified Report

A program of test work was undertaken to provide data on the behavior of projectiles impacting light armor materials, at velocities in the range 1000 ft/sec to 4000 ft/sec. The report includes the results of tests of spherical and cylindrical aluminum projectiles impacting aluminum plates and similar projectiles impacting a light armor built-up out of corrugated aluminum sheets. It concludes with a description of a new method for determining material properties at high speed rates. This method was used to obtain estimates of the yield stress of 2024 T4 aluminum at strain rates from 2900/sec to 13,600/sec.

UNCLASSIFIED

1. Impact - light armor
2. Contract DA-19-129-QM-1574

AD _____ Accession No. _____

Beckman & Whitley, Inc., San Carlos, Calif.
PHENOMENA OF PENETRATION IN LIGHT WEIGHT PERSONNEL ARMOR MATERIALS - J. W. Corcoran and J. M. Kelly

Final Report, 12 Dec. 61, 59 pp., 16 illus., 5 tables.
(Contract DA-19-129-QM-1574) Proj. 7-80-05-001
Unclassified Report

A program of test work was undertaken to provide data on the behavior of projectiles impacting light armor materials, at velocities in the range 1000 ft/sec to 4000 ft/sec. The report includes the results of tests of spherical and cylindrical aluminum projectiles impacting aluminum plates and similar projectiles impacting a light armor built-up out of corrugated aluminum sheets. It concludes with a description of a new method for determining material properties at high speed rates. This method was used to obtain estimates of the yield stress of 2024 T4 aluminum at strain rates from 2900/sec to 13,600/sec.

UNCLASSIFIED

1. Impact - light armor
2. Contract DA-19-129-QM-1574

AD _____ Accession No. _____

Beckman & Whitley, Inc., San Carlos, Calif.
PHENOMENA OF PENETRATION IN LIGHT WEIGHT PERSONNEL ARMOR MATERIALS - J. W. Corcoran and J. M. Kelly

Final Report, 12 Dec. 61, 59 pp., 16 illus., 5 tables.
(Contract DA-19-129-QM-1574) Proj. 7-80-05-001
Unclassified Report

A program of test work was undertaken to provide data on the behavior of projectiles impacting light armor materials, at velocities in the range 1000 ft/sec to 4000 ft/sec. The report includes the results of tests of spherical and cylindrical aluminum projectiles impacting aluminum plates and similar projectiles impacting a light armor built-up out of corrugated aluminum sheets. It concludes with a description of a new method for determining material properties at high speed rates. This method was used to obtain estimates of the yield stress of 2024 T4 aluminum at strain rates from 2900/sec to 13,600/sec.

UNCLASSIFIED

1. Impact - light armor
2. Contract DA-19-129-QM-1574

AD _____ Accession No. _____

Beckman & Whitley, Inc., San Carlos, Calif.
PHENOMENA OF PENETRATION IN LIGHT WEIGHT PERSONNEL ARMOR MATERIALS - J. W. Corcoran and J. M. Kelly

Final Report, 12 Dec. 61, 59 pp., 16 illus., 5 tables.
(Contract DA-19-129-QM-1574) Proj. 7-80-05-001
Unclassified Report

A program of test work was undertaken to provide data on the behavior of projectiles impacting light armor materials, at velocities in the range 1000 ft/sec to 4000 ft/sec. The report includes the results of tests of spherical and cylindrical aluminum projectiles impacting aluminum plates and similar projectiles impacting a light armor built-up out of corrugated aluminum sheets. It concludes with a description of a new method for determining material properties at high speed rates. This method was used to obtain estimates of the yield stress of 2024 T4 aluminum at strain rates from 2900/sec to 13,600/sec.

UNCLASSIFIED

1. Impact - light armor
2. Contract DA-19-129-QM-1574

Beckman & Whitley INC.
SAN CARLOS, CALIFORNIA

PHENOMENA OF PENETRATION
LIGHT WEIGHT RIGID
PERSONNEL ARMOR MATERIALS

Final Report (Part A)

Dept. of Army
Quartermasters Research and
Engineering Command

Contract DA-19-129-QM-1574

Beckman & Whitley, Inc.
Research & Development Division

December 12, 1961

RD 63

By:
J. W. Corcoran
J. M. Kelly

Beckman & Whitley INC.
SAN CARLOS, CALIFORNIA

TABLE OF CONTENTS

TABLE OF FIGURES

Beckman & Whitley INC.
SAN CARLOS, CALIFORNIA

ABSTRACT

A program of test work was undertaken to provide data on the behavior of projectiles impacting light armor materials, at velocities in the range 1000 ft/sec to 4000 ft/sec. The report includes the results of tests of spherical and cylindrical aluminum projectiles impacting aluminum plates and similar projectiles impacting a light armor built-up out of corrugated aluminum sheets. It concludes with a description of a new method for determining material properties at high strain rates. This method was used to obtain estimates of the yield stress of 2024 T4 aluminum at strain rates from 2900/sec to 13,600/sec.

LIST OF TABLES

I. Introduction

Tests have been carried out to study the behavior of light armor materials subjected to high speed impact. The tests fall into two main classes, one concerned with the penetration of the armor material by the projectile, the other being a study of simulated wound damage using gelatin. The final report has thus been divided into two separate sections, the first being the armor penetration study and the second section covering the gelatin cavitation study.

The study of impact processes has received increasing attention in recent years. The physical phenomena associated with the impact process such as cratering, spalling and penetration are, at least qualitatively, understood. Extensive data has been obtained from experimental work which enables empirical formulae to be fitted to these phenomena.

Conversely, the level of theoretical work is not yet very great due to the complexity of the mechanics of the impact process. The impact of a solid projectile on a target leads to a complex combination of elastic and plastic deformation, fluid flow and, for extremely high velocities of impact, explosive conditions. For different impact velocities (see Hopkins and Kolsky (1),) one or more of these various types of behavior will be dominant and it is

convenient to subdivide the process into sections dependent on the type of mechanical behavior which predominates. For a particular choice of projectile material and target material these sections can be associated with a range of impact velocity and the following table gives examples:

	Type of Impact	Velocity * Range
1	Elastic	$0 < V < 200$ f.p.s.
2	Plastic	$200 < V < 2000$ f.p.s.
3	Hydrodynamic	$2000 < V < 16000$ f.p.s.
4	Sonic	$16000 < V < 28000$ f.p.s.
5	Explosive	$28000 < V < 80000$ f.p.s.

* For Aluminum on Aluminum impact.
All figures approximate.

The tests which have been carried out under this contract fall into the plastic regime in the case of the aluminum plate tests and into the hydrodynamic regime in the gelatin tests.

In the elastic regime the stresses nowhere exceed the elastic limit. The impact velocities are low and if the target body is of bounded extent the elastic waves set up in it serve, by means of multiple reflections at the target boundaries, to

produce a quasi-static stress distribution in a time which is of the order of the impact duration. It has been shown by Hunter (2) that not more than 1% of the available kinetic energy of the projectile is lost during elastic impact and the remainder, stored as elastic strain energy, is restored to the projectile causing it to rebound.

In the plastic regime a portion of the kinetic energy of the projectile is converted into heat by plastic deformation. As the velocity of impact increases this portion becomes a progressively larger percentage of the incident kinetic energy and the influence of the elastic deformation less. For aluminum on aluminum impact this regime extends from 200 ft/sec to 2000 ft/sec.

Most of the analyses which are available for problems in this regime have used the rate independent theory of placticity, a theory which has been so successful for static problems that attempts have been made to extend it to dynamic problems. It has been applied to the impact of rods on rigid blocks and to the behavior of beams struck by projectiles. It has proved useful only in these simplified cases; its extension to more complex problems has shown serious shortcomings, mostly related to the assumption that the yield stresses are independent of strain rate. It is known that the yield strength of metals is sensitive to the strain

rate. To improve on the analysis some authors have added a viscous term to the perfectly plastic model. A summary of analyses of this kind is given by Cristescu (3) and Goldsmith (4).

Concurrent with the experimental work reported here, is a theoretical study of dynamic plastic deformation by L. E. Fugelso (5) of American Machine and Foundry Corp.

In this, Fugelso has obtained analytical and numerical solutions for the behavior of a half space subjected to impact by a cylindrical projectile using, as the mathematical model of material behavior, the assumption that the material deforms, first due to elasticity of the body and following this due to the motion of dislocations under the applied stress. Thus the medium exhibits an instantaneous elastic strain and a time dependent plastic deformation. An analysis based on such a model is not subject to the disadvantages of the rate independent plastic analyses. Its use in predicting crater formation is restricted to cases where convection of material from the immediate zone of the impact is not large. However it may still be applied to regions outside this zone even if considerable convection is present.

In the hydrodynamic regime the resistance offered by the target to the projectile depends to a much greater extent on its inertia than on its shear

strength. The stresses which are induced exceed the yield stresses so much that the rigidity of the material may be neglected and the material considered as an incompressible fluid.

It has been found that this concept is a useful one and may be used over a wide range of velocities. The lowest velocity of the range is the maximum velocity for which the plastic regime applies and the highest velocity is usually taken as the velocity of dilatational stress waves in the target material.

When the velocity of the projectile exceeds the speed of dilatational waves in the target material a new regime appears, in which the target material is treated as a compressible fluid. In this regime a true shock will occur. The analysis of problems in this regime has been hampered by lack of a suitable equation of state for metals. However experimental work by Rice, Walsh and McQueen, (6), has provided much data in this field and a pioneering analysis by Bjork (7) is available. When the impact velocity becomes large compared with the sonic velocity the quantity of kinetic energy available for conversion to heat is large, being adequate to melt and vaporize the projectile and the portion of the target immediately adjacent to it. This vaporized metal is compressed in the target until the projectile is completely imbedded.

Fig. 1.1 Color Schlieren Record of Impact of Aluminum Cylinder on Lucite Block. Initial velocity of projectile 3300 ft/sec. Interval between frames 3.33 μsec.

The subsequent expansion is equivalent to an intense explosion within the target, hence the name of this regime. Hopkins and Kolsky give its initiation as approximately three times the sonic speed of the target material. We will not discuss these two regimes further as they are much beyond the limits of the experimental work performed under this contract.

The principal phenomena occuring during an impact are illustrated in Fig. 1.1. A cylindrical aluminum projectile traveling at 3000 ft/sec is shown impacting a block of lucite. (A transparent target is used to permit observation of the propagation of the various stress waves.) The picture is taken with a novel color schlieren technique (Fig. 1.2) which indicates the amount and direction of the deflection of light waves passing through the target. The use of this technique permits unambiguous identification of these waves.

The impact generates a longitudinal (or dilatational) wave and transverse (or shear) wave. At its point of contact with the surface the longitudinal wave generates a shear wave known as a head or trailing wave which is tangential with the spherical shear wave. Fig. 1.3 illustrates diagramatically these waves and should be compared with the photographs. The shear zone is seen to be extremely

FIG. 1.2. OPTICAL ARRANGEMENT FOR COLOR SCHLIEREN RECORDS

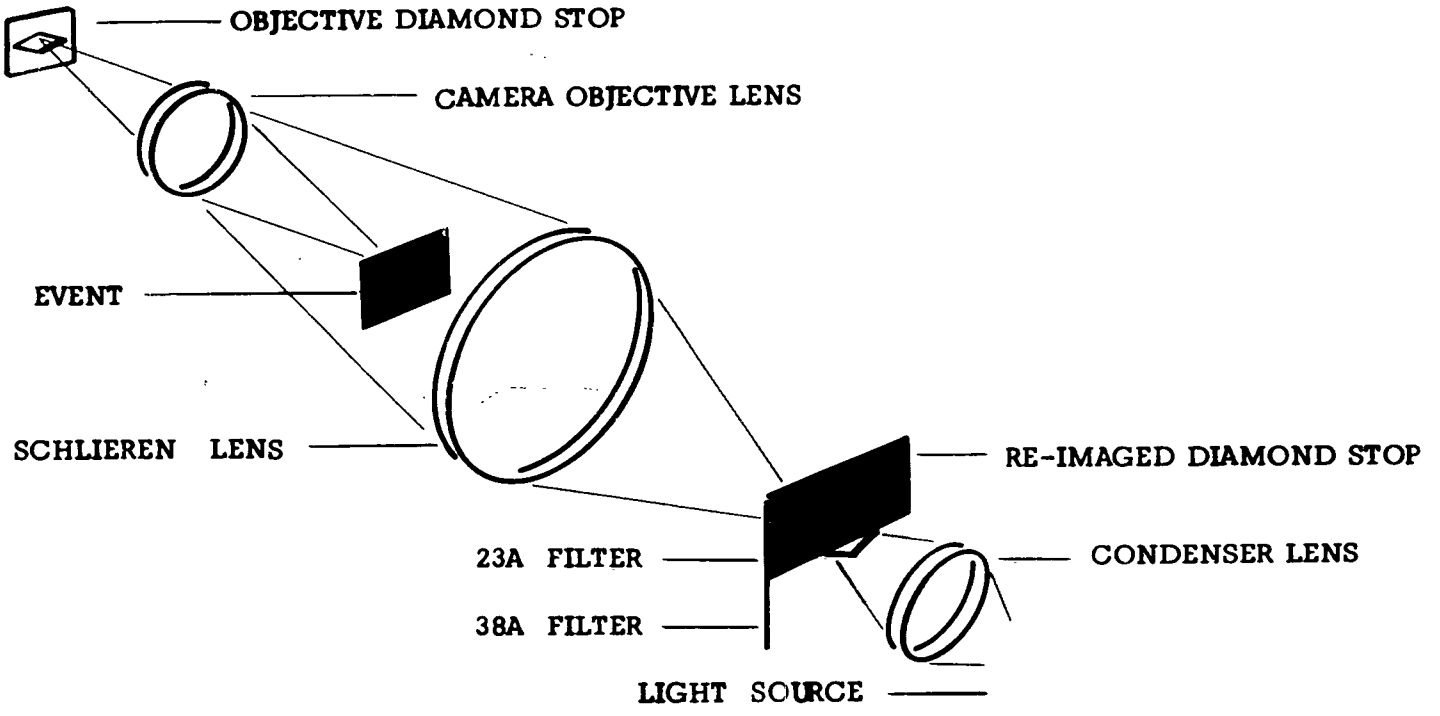

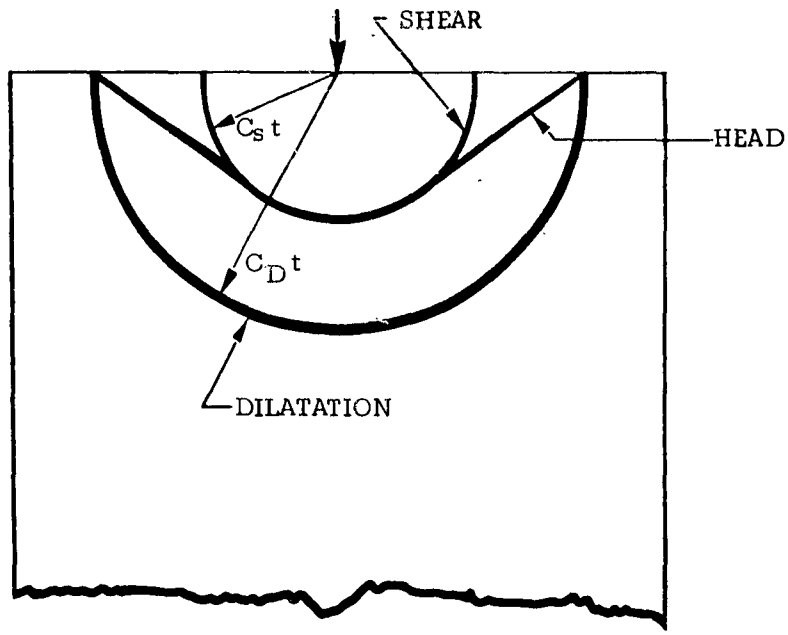

FIGURE 1.3 DILATATIONAL AND SHEAR WAVES IN IMPACTED BLOCK

opaque probably due to considerable fracture in this region.

Fig. 1.1 may be considered a qualitative confirmation of the mathematical model developed by L. E. Fugelso for the study of impacts.

II. Aluminum Plate Tests

The first phase of the work under this contract consisted of the study of the impact of projectiles in the velocity range 1000 to 4000 ft/sec. The studies involved both spherical and cylindrical aluminum projectiles striking aluminum plates.

The projectiles were fired from a .300 Magnum rifle. The cylinders were .300 in. diameter by .300 in. long, and the spheres were .300 in. diameter. A typical record obtained with the Dynafax camera is shown in Fig. 2.1.

Data obtained from a series of such shots is given in Table I. The impact velocity, the velocity of the projectile after impact, the target velocity and the spall velocity, if any, were determined from these photographs. From this data, it was possible to construct a momentum balance. It may be seen from the Table that the bulk of the momentum is transferred to the target plate. The difference of the sum of the momenta from zero is generally a few percent and this is probably due to errors of measurement of the target plate velocity. This was so low that its motion was barely perceptible.

An analysis of the energy balance indicates that about 98% goes into plastic work on the target and projectile. The residual kinetic energy of the pro-

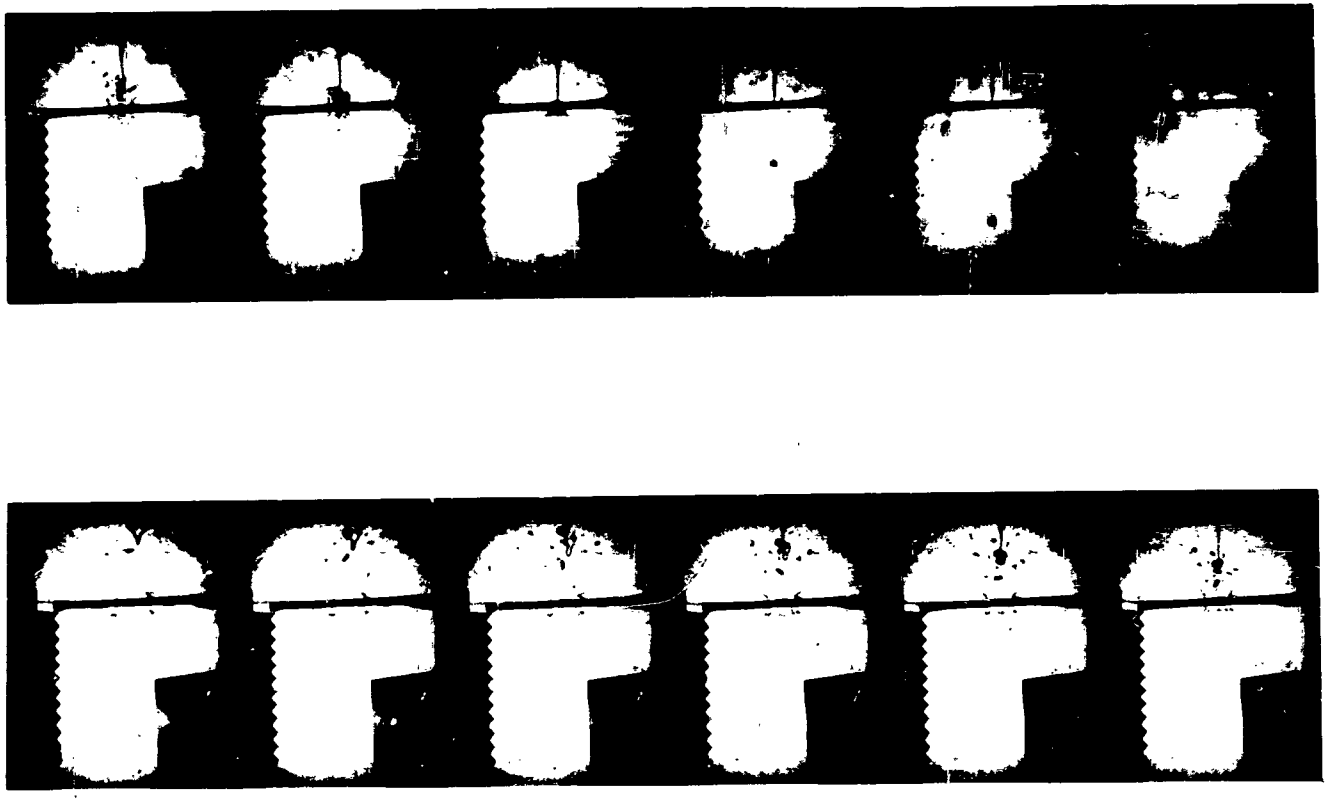

Fig. 2.1 Dynafax Record of Projectile Impact on Aluminum Plate (Shot No. 28). Interval between frames, 56 usec.

TABLE 1 ANALYSIS OF DIVISION OF ENERGY AND MOMENTUM DURING IMPACT

SHOT No.		26	27	30	32	31	28	29
PROJECTILE								
Type		0.3in.Dia.Sphere		0.3in.Dia.x0.3in.long Cylinder				
Weight	pounds	.00138	.00138	.00207	.00207	.00207	.00207	.00207
Initial velocity	ft/sec	2880	3440	1430	1960	2140	3360	3400
Residual velocity	ft/sec	-160	-220	-135	-140	-189	+680	-94
Maximum elastic strain	%	0.94	1.29	0.79	0.82	1.11		0.55
TARGET								
Type		6"x6"x1/4"		4"x4"x1/4"			6"x6"x1/4"	6"x6"x3/8"
Weight	pounds	0.875		0.390			0.875	1.315
Velocity	ft/sec	5.1	5.6	11.0	12.6	12.7	5.7	4.6
Depth of penetration	inch	0.110	0.178	.0235	0.050	0.059	penetrated	0.100
MOMENTUM BALANCE								
Projectile								
Initial	pound sec	0.123	0.1475	0.0919	0.1260	0.1380	0.216	0.218
Residual	pound sec	-0.0068	-0.0094	-0.0087	-0.0090	-0.0121	+0.0437	-0.0060
Target	pound sec	0.138	0.152	0.1358	0.1326	0.1540	0.1550	0.1880
Net	pound sec	+0.008	-0.005	+0.0362	+0.0176	+0.0039	-0.0170	0.0360
Net as % of initial		+6.5	-3.2	+38.0	+13.5	+2.8	-7.8	-16.5
ENERGY BALANCE								
Projectile								
Initial	pound-ft	178	254	65.9	124	147.5	363	372
Residual	pound-ft	0.55	1.04	0.58	0.63	1.15	27.3*	0.28
Target	pound-ft	0.34	0.41	0.76	0.96	0.97	0.42	0.25
Plastic work	pound-ft	177.1	252.7	64.6	122.4	145.4	325.3	371.5
SHOCK STRAIN (Eq. 2.3)	%	8	9.5	3.9	5.5	5.9	9.3	9.4
SHOCK PRESSURE (Eq. 2.2)	k.s.i.	933	1130	469	642	702	1100	1110
ESTIMATED AVERAGE STRESSES								
Compressive (Eq. 2.5)	k.s.i.	274	242	460	415	420		630
Shear	k.s.i.			140	125	126		126
TIME OF IMPACT (Eq. 2.6)	μsec.	6.4	8.25	2.80	4.22	4.66		4.90

* INCLUDES SPALL

Beckman & Whitley INC. SAN CARLOS, CALIFORNIA

jectile and target amount to 1%, and the elastic and vibrational energies are estimated to be of a comparable order. From the modulus of resilience using the limiting elastic strain observed in the projectile, the maximum elastic energy which can be stored in a unit volume is

$$U = \frac{1}{2} \epsilon^2 E = 320 \text{ in lb/in}^2 \qquad (2.1)$$

If a volume is taken equal to that of the bullet plus the part of the target immediately beneath it, this amounts to 1.25 ft.lb. or significantly less than that of any projectile.

To assess the stresses and strains developed in the target and projectile, two essentially independent calculations are possible:

1. From the Hugoniot-Rankine equations for shock waves it can be shown that when similar metals collide, the pressure, P, at the head of the shock wave is:

$$P = \frac{1}{2} p_o v_o D \approx \frac{1}{2} p_o v_o c \qquad (2.2)$$

where the sound speed, c, may be used instead of the shock speed, D, providing the shock is weak. A shock may generally be considered weak if the particle velocity is a small fraction of

the material sound speed, and this is true in these experiments.

Similarly the compression, $\Delta V/V_o$, which for plane shocks is equivalent to a one directional strain, ϵ, is given by

$$\frac{\Delta V}{V_o} = \epsilon = \frac{v}{D} \approx \frac{v}{c} \tag{2.3}$$

Both shock pressure and strain are shown in the table.

2. From the depths of penetration, x, observed in the target, and the initial energy of the projectile, it is possible to estimate an average force, $\overline{F}$, necessary to stop the projectile:

$$\overline{F}x = \frac{1}{2} mv^2 \tag{2.4}$$

and hence an average stress across the cross-sectional area of the projectile, A:

$$\overline{S} = \frac{mv^2}{2Ax} \tag{2.5}$$

It may be seen from the Table that the average compressive stress is about 70% of the shock pressure for cylindrical projectiles and about 25% for

spherical projectiles. Such a difference is to be expected because of the effect of side rarefaction waves, which decrease the shock strength in the vicinity of the point of impact, and because of the rarefaction waves from the rear of the target plate which cause additional forward motion, and hence an additional displacement of the target surface. The effect of side rarefactions should be more pronounced in the spherical geometry than in the cylindrical. It may therefore be said that compressive stresses in impacts may generally be estimated on the basis of simple shock theory, and that the depth of penetration permits an estimate of the average stress over the period of impact.

The duration of impact computed from the initial momentum and the average compressive stress gives durations of impact of about 4 μsec. This is in close agreement with times estimated for a shock wave to pass up the projectile and a rarefaction to return to the projectile-target boundary:

$$t = \frac{2h}{c} = 3 \text{ μsec} \qquad (2.6)$$

(The bar velocity, 17,000 ft/sec, is used because there is no lateral constraint.)

The target thickness used in these tests was chosen so that in most cases penetration just failed to occur. The projectiles were reflected with velocities

ranging from 95 to 220 ft/sec. From this velocity, the limiting elastic strain in the projectile may be estimated. Consider a cylindrical projectile which has been just brought to rest by the resistance of the target. Up till this time, the target has been applying a force to the front of the projectile causing a compressive stress within it. Upon the cessation of motion this stress is relieved inducing a backward motion of the projectile. The elastic strain energy is transformed into kinetic energy:

$$1/2\ E\epsilon^2 = 1/2\ \rho v^2$$

or

$$V = \epsilon \sqrt{\frac{E}{\rho}} = \epsilon c \qquad (2.7)$$

where c is the bar sound velocity, 17,000 ft/sec for aluminum and ϵ is the maximum strain in the projectile. The basic hypothesis is that the compressive stress is relieved along a Hooke's Law curve.

In Fig. 2.2 the elastic strain is plotted is a function of initial velocity. From the limited amount of data it would appear that the elastic strain has a maximum value of 1.1% for impact velocities of about 2500 ft/sec.

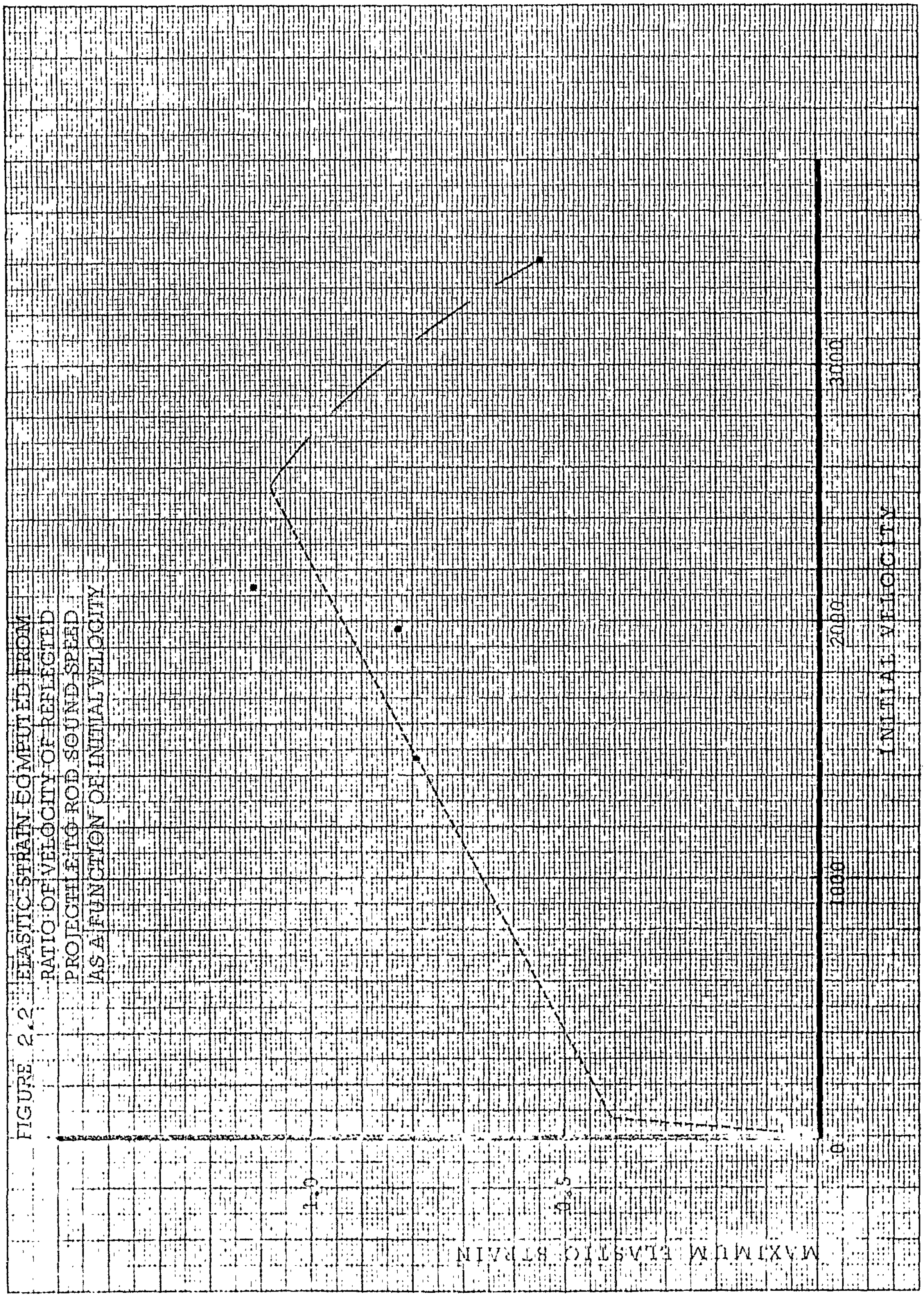

FIGURE 2.2 ELASTIC STRAIN COMPUTED FROM RATIO OF VELOCITY OF REFLECTED PROJECTILE TO ROD SOUND SPEED AS A FUNCTION OF INITIAL VELOCITY

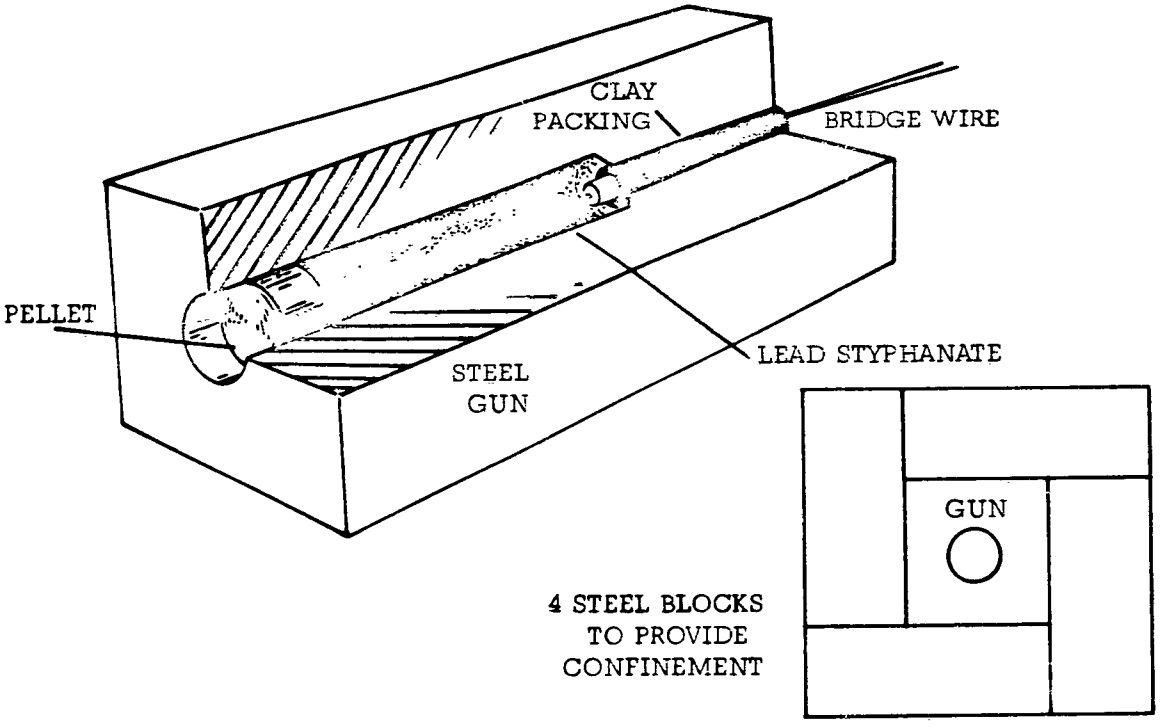

FIGURE 2.3 EXPLOSIVE PROJECTILE LAUNCHER

Beckman & Whitley INC.
SAN CARLOS, CALIFORNIA

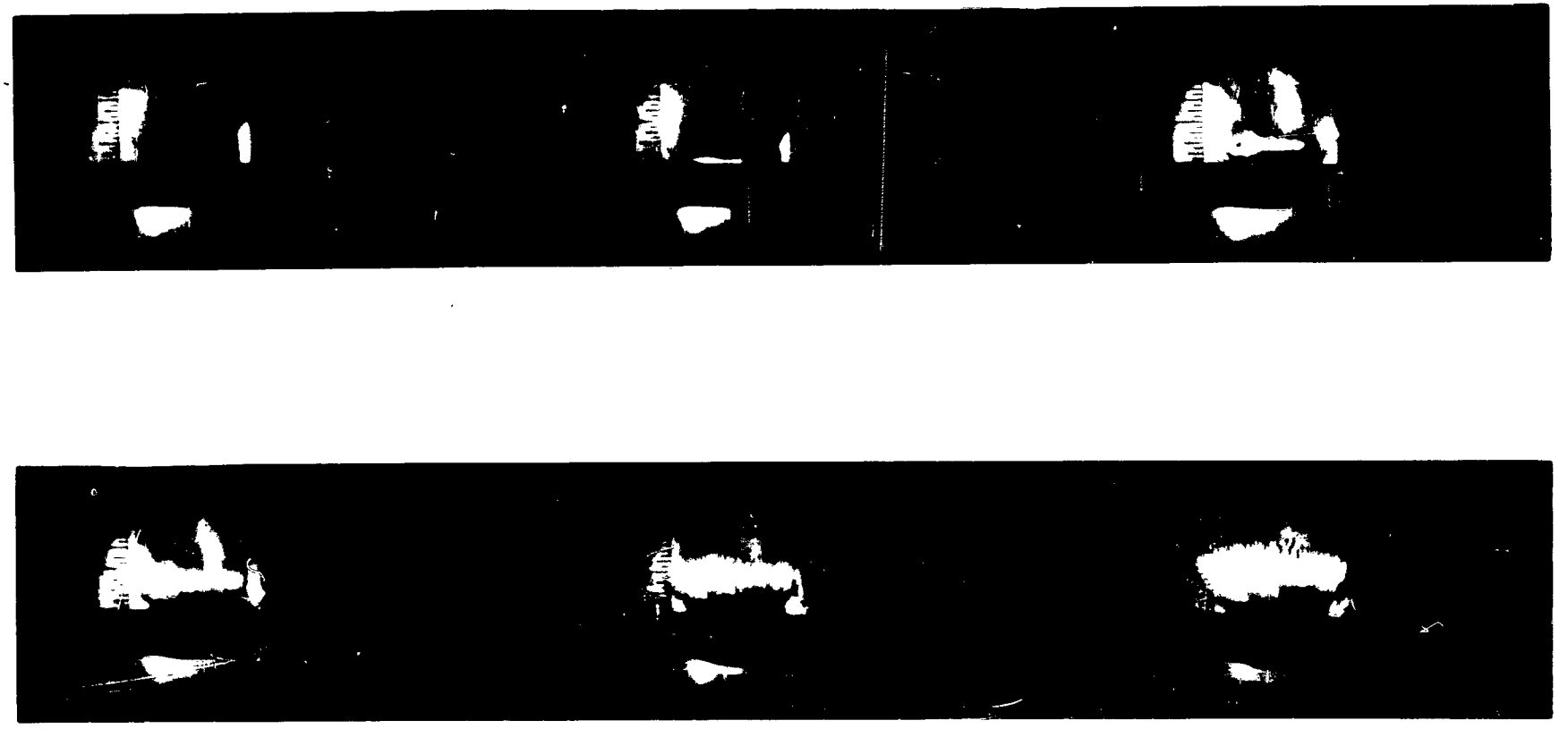

Fig. 2.4 Framing Camera Record of Projectile Impact on Aluminum Plate used to Determine Free Surface Velocity (Shot No. 73). Interval between frames, 4.11 usec.

A PROJECTILE
C PLATE
E&F AIR SHOCK

B AIR SHOCK
D JET
G REAR SURFACE MOTION

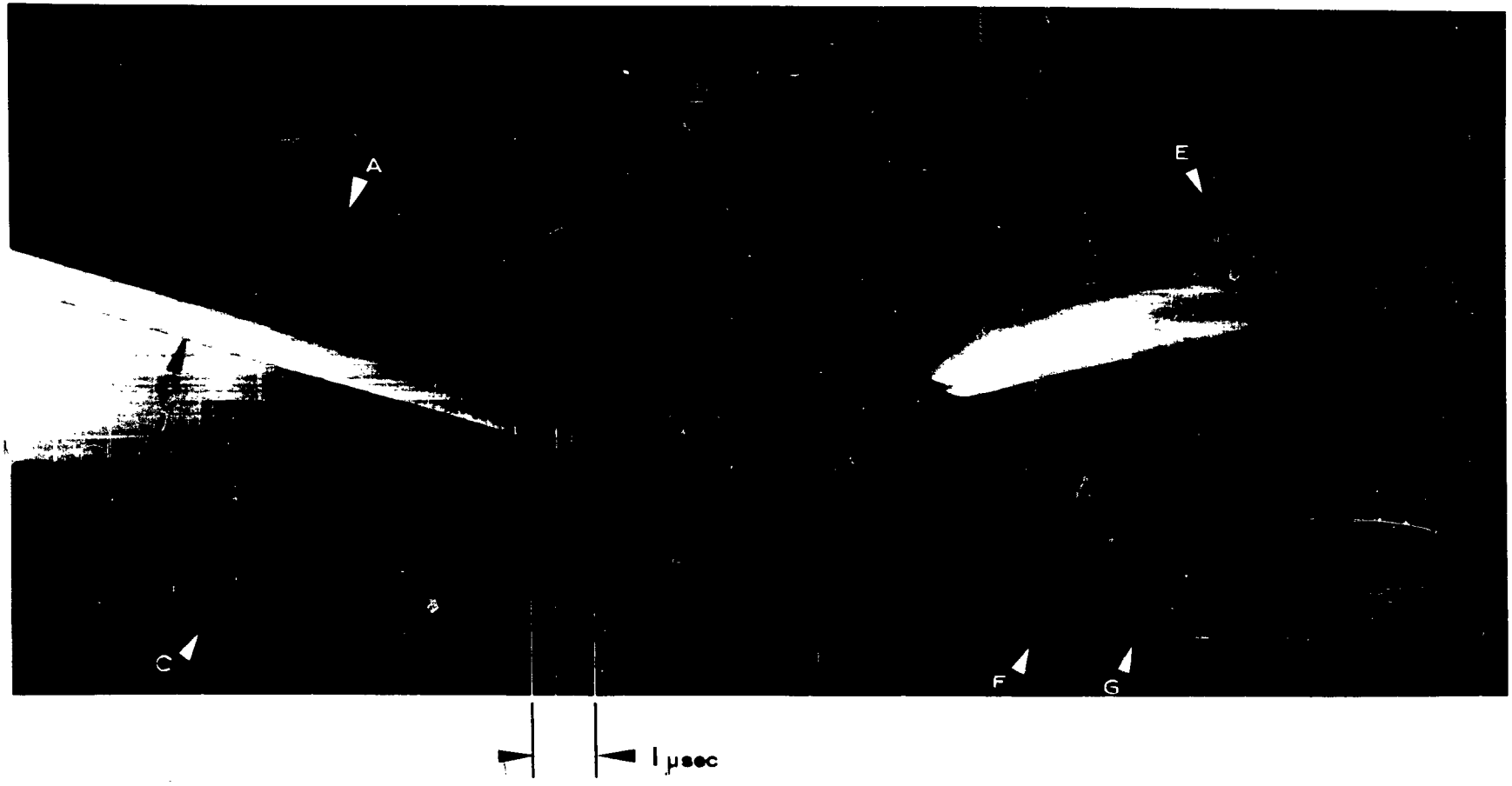

Fig. 2.5 Streak Camera Record of Projectile Impact on Aluminum Plate (Shot No. 75) The initial velocity of the rear surface permits determination of pressure of the transmitted shock. This type of picture gives a continuous record of events along a single line in the framing record, Fig. 2.4.

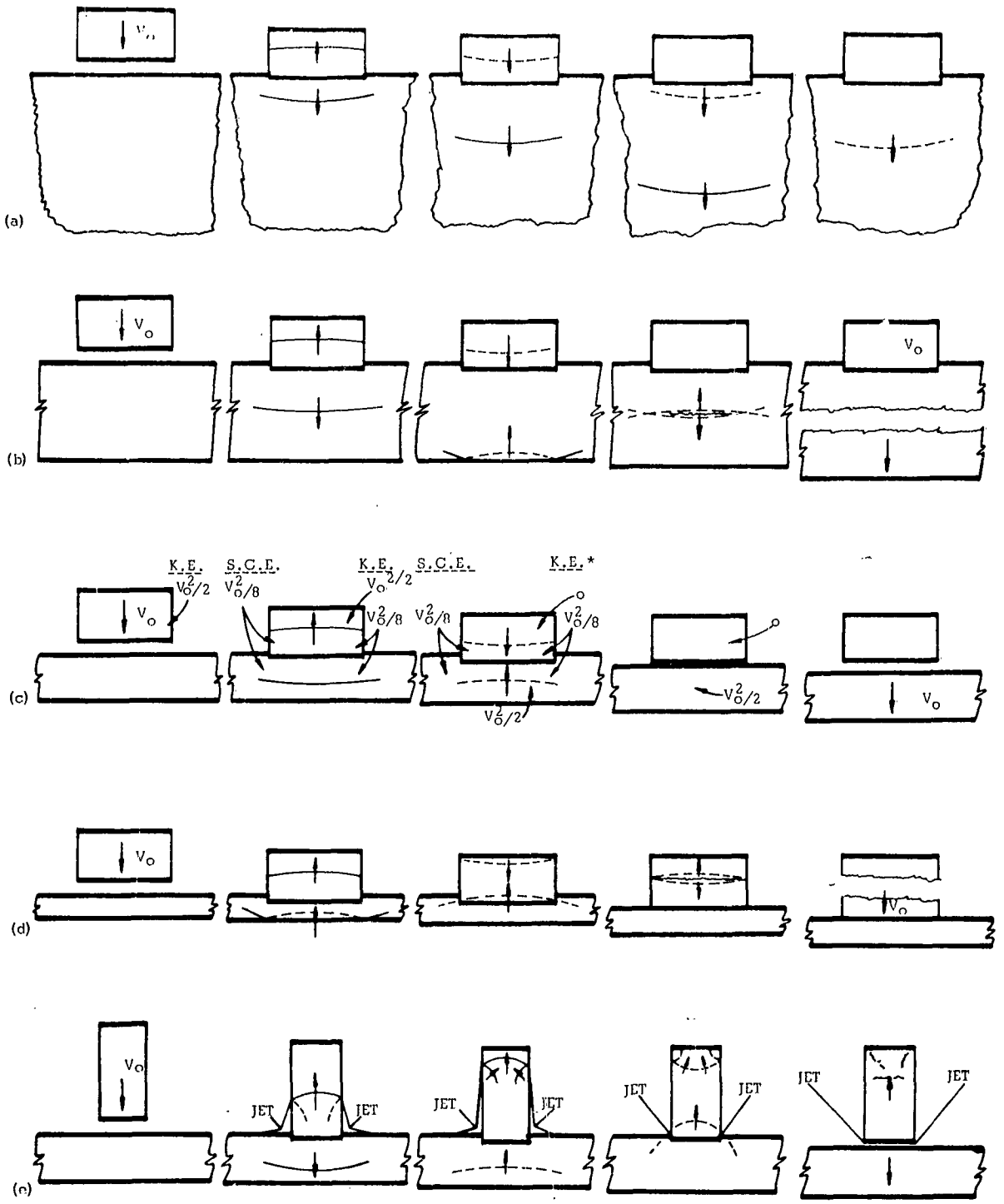

(a) PROJECTILE INTO HALF SPACE
(b) PROJECTILE INTO THICK PLATE
(c) PROJECTILE INTO PLATE OF SAME THICKNESS
(d) PROJECTILE INTO THIN PLATE
(e) LONG NARROW PROJECTILE

*K.E. - KINETIC ENERGY
S.C.E. - SHOCK COMPRESSION ENERGY
——— SHOCK WAVE
– – – RAREFACTION WAVE

FIGURE 2.6 SHOCK PROPOGATION IN IDEALIZED IMPACT OF TWO SIMILAR MATERIALS

In addition to these studies with the Dynafax camera, pictures were taken with the Model 189 Framing camera and a Model 339 streak camera to assess the phenomena occurring during the brief duration of impact, about 4 μsec. This is impossible to achieve using a rifle because of the uncertainty in time of arrival of the projectile at the target. To circumvent this difficulty, an explosive projectile launcher was designed. (Fig. 2.3)

The projectile is imparted a velocity which may be adjusted by varying the amounts of explosive. Because of the high, and reproducible, rate of detonation of the explosive, it is possible to predict the time of arrival of the projectile at the target within a few microseconds, which is necessary to achieve proper synchronization with the camera.

A series of pictures from a Framing camera record are shown in Fig. 2.4, and a streak record is shown in Fig. 2.5. The latter gives a continuous time recording of the events occurring on one line through the projectile and along its trajectory.

To assist in interpretation of these records, the various shock phenomena occurring during an impact are presented in an idealized form in Fig. 2.6.

It is assumed that both target and projectile are the same material, hence the particle velocity within the shock zone is exactly 1/2 the initial speed of the projectile. (Dissimilar materials can also be treated by impedance matching techniques in a more complex way.) Also, in the first four figures, the effects of rarefactions from the peripheral corners of the bullet are omitted to simplify the approach; i.e., the shocks are treated as essentially planar. The fifth figure indicates the effect of the rarefactions.

The general sequence of phenomena occurring during an impact of a broad projectile on an infinite half space are shown in Fig. 2.6a. Upon collision, one shock wave is propagated into the target and a second back into the projectile. The initial energy of the projectile is divided into four equal parts. The target is imparted a kinetic energy per unit mass of $v_o^2/8$ and a similar amount of compressive energy. The kinetic energy per unit mass of the projectile, in the zone between the interface and the second shock is reduced to $v_o^2/8$ and it also contains the same amount of compressive energy. When the shock wave is reflected from the rear surface of the projectile, as a rarefaction wave, it decompresses the projectile and leaves it with zero velocity. The rarefaction then follows the shock into the target and the initial energy is transmitted as a

pressure pulse with an associated kinetic energy of motion. The distance from the shock to the trailing wave is twice the length of the bullet.

In the second sequence the effect of the rear surface of the target is indicated. When the shock wave reaches this surface it is reflected as a tensile or a rarefaction wave. Internal cavitation or spalling is induced by such waves if they exceed the tensile yield stress of the target.

When this wave meets the similar wave from the rear of the projectile, a zone of even greater tension develops. This may occur within the projectile, at the projectile-target interface, or within the target, depending on whether the projectile is longer than, equal to, or thinner than the target. The second, third and fourth sequences indicate these effects.

Where the shocks move along a free surface, the material is free to move laterally and lose its shock compression. This generates a rarefaction wave which moves into the previously shocked zone. This effect is illustrated in the fifth sequence. It is primarily because of these waves that the original shock cannot remain plane, and decreases in strength.

The laterally expanding material from the bullet and the plate collide in the peripheral zone around

the area of impact. This induces a conical jet by the same hydrodynamic mechanism occurring in shaped charges. This jet moves at a speed of twice the original projectile velocity.

This jet rapidly obscures the projectile, preventing direct photographic observation of the shock waves propagating backward through it. The presence of the jet, however, confirms their existence.

The high speed camera records permit a determination of the initial velocity of the rear face of the target plate, as well as the velocity of the projectile. By use of the data of Rice, McQueen & Walsh (6) and the Hugoniot-Rankine equations it is possible to determine the pressure of the incident and transmitted shock wave in the target plate, Table II.

It may be noted that while the pressure at the point of impact in a typical shot is 1550 ksi, the pressure at the rear surface is reduced to 171 ksi. This reduction is due to the combined effects of spherical divergence and the rarefaction waves which emanate at the periphery of the bullet.

It is pertinent to note that, at the shock pressures of interest in these impacts, aluminum develops a double wave configuration as described

TABLE 11 SHOCK PRESSURES AT POINT OF IMPACT AND TRANSMITTED THROUGH THE TARGET

SHOT No.	73	75	77
CAMERA	Model 189 framing camera	Model 339 streak	Model 339 streak
PROJECTILE Type Velocity ft/sec	Cyl.1/4"x1/2"dia. 3880	Cyl.1/4"x1/2"dia. 3880	Cyl.1/4"x1/2"dia. 4000
TARGET PLATE Type Free surface velocity ft/sec	4"x4"x1/2" 614	4"x1"x7/16" 850	4"x1"x1/2" 505
SHOCK PRESSURES Projectile-target interface Transmitted pressure	1470 k.s.i. 207 k.s.i.	1470 k.s.i. 290 k.s.i.	1550 k.s.i. 171 k.s.i.

Buckmaster & Whitley INC.
SAN CARLOS, CALIFORNIA

by Fowles (8).

The first wave is an elastic wave which transmits a peak pressure depending on the yield strength of the material. The second wave is a plastic wave propagating at a lower velocity than the elastic wave. As the shock pressure increases the plastic wave velocity reaches the value of the elastic wave velocity and the two wave structure disappears.

The value of the elastic shock pressure may be estimated in the following way. The stress-strain relation for an elastic solid is:

$$\sigma_{ij} = 2\mu\epsilon_{ij} + \lambda\epsilon_{kk}\,\delta_{ij}$$

where σ_{ij} is the stress tensor
ϵ_{ij} is the strain tensor
δ_{ij} is the kronecker delta
and μ, λ are the Lamé elastic constants of the material.

Since the stress state in a plane shock is uniaxial compression, the stress tensor takes the form

$$\sigma_{ij} = \begin{pmatrix} (2\mu + \lambda)\,\epsilon_{11} & 0 & 0 \\ 0 & \lambda\epsilon_{11} & 0 \\ 0 & 0 & \lambda\epsilon_{11} \end{pmatrix} \qquad (2.9)$$

The Tresca, or maximum shear stress, yield condition in this notation takes the form

$$\left|\sigma_{11} - \sigma_{22}, \sigma_{33}\right| < Y \tag{2.10}$$

where is the yield stress in simple tension.

Hence $$((2\mu + \lambda) - \lambda)\epsilon_{11} = -Y \tag{2.11}$$

When yielding commences $$\epsilon_{11} = -\frac{Y}{2\mu} \tag{2.12}$$

Thus P_e the elastic shock pressure, is given by

$$P_e = -\sigma_{11} = \frac{(2\mu + \lambda)}{2\mu} Y \tag{2.13}$$

For 2024 Al the values of μ, λ, Y are approximately as follows:

$$\mu = 2.5 \times 10^{-10} \text{ newtons/m}^2$$

$$\lambda = 6.1 \times 10^{-10} \text{ newtons/m}^2$$

$$Y = 40{,}000 \text{ p.s.i.}$$

Thus

$$P_e = 88{,}800 \text{ p.s.i.} \tag{2.14}$$

The difference in velocity between this elastic wave and the plastic shock wave is extremely small. It is at its maximum where the plastic wave has its least intensity which, due to the effects of spherical divergence and rarefactions already discussed, occurs at the lower face of the target. Here the difference is only between 5.45 mm/μsec for the shock velocity and 6.4 mm/μsec for the elastic wave velocity. The difference in the time of transmission of the two waves through the 1/2" thick plate will thus be 0.3 μsecs, which is not detectable in the record.

Perhaps the most striking phenomena indicated in Table I is the large amount of energy absorbed by the target and projectile. The energy absorbed per unit volume has been computed on the basis that this volume is that of the projectile plus a volume of plate twice the projectile diameter and normal thickness. Inspection of target plates indicates this is a reasonable estimate of the zone affected by the impact. These quantities are given for the more energetic impacts in Table III.

TABLE III

Shot No.	Energy Vol. in lb/in^3	Temperature Rise °C.
31	18,900	51
28	42,500	114
29	35,000	94

A typical value for the energy absorption of 2024 aluminum at low strain rate is 9000 in-lb/in^3, or about one fourth that observed. It should be noted that tests 28 and 29 are at similar velocities, 3400 ft/sec, and that the first target was penetrated and the second, which was thicker (3/8" vs 1/4") was not.

The temperature rises corresponding to the plastic work have been computed and are also shown in Table III. An attempt was made to measure such rises experimentally by using Tempilaq paint on the rear surface of the target. Exposure to temperatures above a specified value causes an irreversible chemical reaction which is indicated by color change in the paint. No such change was observed in these tests. The only explanation at present is that the temperature drops by conduction too rapidly for the chemical change to occur.

III. Corrugated Armor

A great deal of development work has been done on light weight structures for aircraft panels. A common structural form is the sandwich plate. Two thin sheets of metal are separated by a lightweight shear core. The yield strength of such panels is of the same order as the yield strength of the solid section of the same depth but its weight is much less. It has been speculated that such structures might be extended to dynamic loading as in lightweight armor. Such an extension is reasonable in the light of experimental work done on what is known as the "Wipple Bumper". It was shown by Olshaker (9) that the penetrating power of a high speed projectile is greatly reduced (by factors up to 1/3) when a thin plate of material is placed before the target. It is conjectured that the impact with the thin plate sets up shock waves in the projectile which tear it apart before it reaches the main target, the individual parts having less penetrating power than the complete projectile.

In an attempt to determine whether such a mechanism could be achieved in built-up armor a small series of tests were performed. Aluminum foil of the household variety was given a corrugated shape by rolling in pinion wire and enough sheets to give a weight per unit area of .025 lb/in^2 (equivalent to a 1/4" sheet of aluminum previously tested) were laid on top of each other, the foils being placed

so that the successive sheets had their corrugations perpendicular. The strength of this material was measured to be 11,000 lb/in^2. Two tests using this material and a third test using 0.012 in. sheets of 2024A1 similarly corrugated were performed.

The projectiles were 0.300" dia. x 0.300" cylinders of 2024 T4 aluminum and the charge was chosen to give a projectile velocity about that which a 1/4 inch aluminum plate would stop. The results of the three tests are included in Table IV.

Clearly, under these test conditions, the corrugated material is less effective than the solid section. On the basis of these tests and in the light of the results of Olshaker it is felt that an improvement in the performance of this type of armor is only possible if the sheets are farther apart and the projectile velocities are higher to allow the mechanism of projectile break up, already mentioned, to take place. It would also appear to be necessary to fix the sheets together by means of a high strength epoxy resin in order to develop transverse shearing stresses in the aluminum. The impact velocity has an important influence on projectile shatter and it is felt that the velocities here are too low for this to take place. The criterion for such failure is that the intensity of the rarefaction waves set up by the reflection of the compression wave at the

TABLE IV ANALYSIS OF CORRUGATED ARMOR RECORDS

SHOT No.	233	234	286	31
PROJECTILE				
Type	.300" dia x .300" lg. Cyl.-2024 Al.			
Weight pound	.00207			
Initial velocity, u_1, ft/sec	2520	2130	2320	2140
Exit velocity, u_2, ft/sec	1230	960	565	0
TARGET				
Material	Aluminum Foil	Aluminum Foil	2024 Alum. Sheet	2024 Alum. Plate
Length in.	8.75	5.25	1.25	0.25
Density lb/in^3	.00286	.00475	.0200	0.0975
STRESSES				
Pressure on projectile - Target interface, p.s.i.	6750	8220	36,200	702,000
Mean retarding stress, p.s.i.	2400	3770	23,000	420,000
VELOCITY RATIO $\frac{u_2}{u_1}$	0.49	0.45	0.24	0

Beckman & Whitley INC. SAN CARLOS, CALIFORNIA

free end of the projectile should exceed the tensile strength of the material.

The shock equations indicate that the compressibility of any material is given by the ratio of the particle velocity to the shock speed

$$\frac{\Delta V}{V_o} = \frac{u}{D} \tag{3.1}$$

If the compressibility of the foils is taken to be unity, then the shock speed must exactly equal the particle velocity. On this basis the Rankine-Hugoniot equations predict that the pressure, P, at the projectile face is

$$P = \rho_o \, uD = \rho_o \, u^2 \tag{3.2}$$

where ρ_o is the density of the target.

The equation of motion of the system is thus

$$m \frac{du}{dt} = -A\rho_o u^2 \tag{3.3}$$

where A is the area of the projectile.

Thus

$$mu \frac{du}{dx} = -A\rho_o u^2 \tag{3.4}$$

which may be integrated to give

$$\log \frac{u_2}{u_1} = - \frac{A\rho_o}{m} \cdot L \tag{3.5}$$

where L is the length of the target and h is the length of the projectile.

Thus

$$\frac{u_2}{u_1} = \exp.\left(-\frac{\rho_o L}{\rho_p h}\right) \tag{3.6}$$

where ρ_p is the density of the projectile.

Since L was chosen to provide a surface density equivalent to a 1/4" solid plate the quantity

$$\frac{\rho_o L}{\rho_p h} = \frac{0.250}{0.300} = 0.875 \tag{3.7}$$

and

$$\frac{u_2}{u_1} = 0.416 \tag{3.8}$$

The resulting velocity ratio of shots No. 233, 234, is close to this and those of shots No. 286, 31, show the effect increasing material rigidity.

IV. Yield Stress Determination at High Strain Rates

It was mentioned in the Introduction that one of the major disadvantages of dynamic plastic analysis has been lack of information on the dependence of yield strength on rate of strain. In impact tests, where the strain rate may be extremely high, this factor can introduce uncertainties in the validity of such an analysis. Nevertheless, surprisingly little experimental data is available on the behavior of metals at high strain rates. The first comprehensive tests appear to have been done by Manjoine (10) using a modification of a standard testing machine. He obtained test rates of up to 10^2/sec but examined only mild steel. Later work was done by Campbell (11) using a machine in which a cylindrical specimen was impacted by a dropping weight. The strains in these tests were measured by electrical resistance gauges. The maximum strain rate obtained was of the order of 15/sec. Aluminum was examined.

The strain rates achieved in these tests are for the most part inadequate for use in problems concerning impact by projectiles or pressure waves on armor plating. Here strain rates in the range of 1000/sec to 10,000/sec are needed and for this range conventional test methods are of little use. The reaction time of any conventional strain measuring device would be greater than the test duration

at such strain rates and hence optical methods of measurement are necessary. In this paper a method will be described which involves such strain rates and which makes use of high speed photographic recording to determine the strain and strain rates.

The method given here was described in a proposal report by J. W. Corcoran (PR 719A, Beckman & Whitley, Inc., Proposal for Experimental Study of Impact and Penetration Phenomenon in Light Armor Materials). It will be useful to describe it in some detail here.

A thin cylindrical shell of the test material is filled with water. A cylindrical explosive charge is located along the center line of the tube. (See Fig. 4.1) The charge is ignited at one end causing a shock wave which moves outward through the water striking the metal and accelerating it radially outwards. The shock wave, on reaching the free surface, reflects with change of sign, propagating a negative pressure wave (a rarefaction) back into the metal. This negative pressure causes the water to cavitate at the metal water interface a very short time after the impact has taken place. This sequence of events is clearly shown in Fig. 4.2, a series of high speed photographs of a longitudinal section of a specimen.

The tube is then separated from the water and moves under its own inertia losing kinetic energy by plastic deformation.

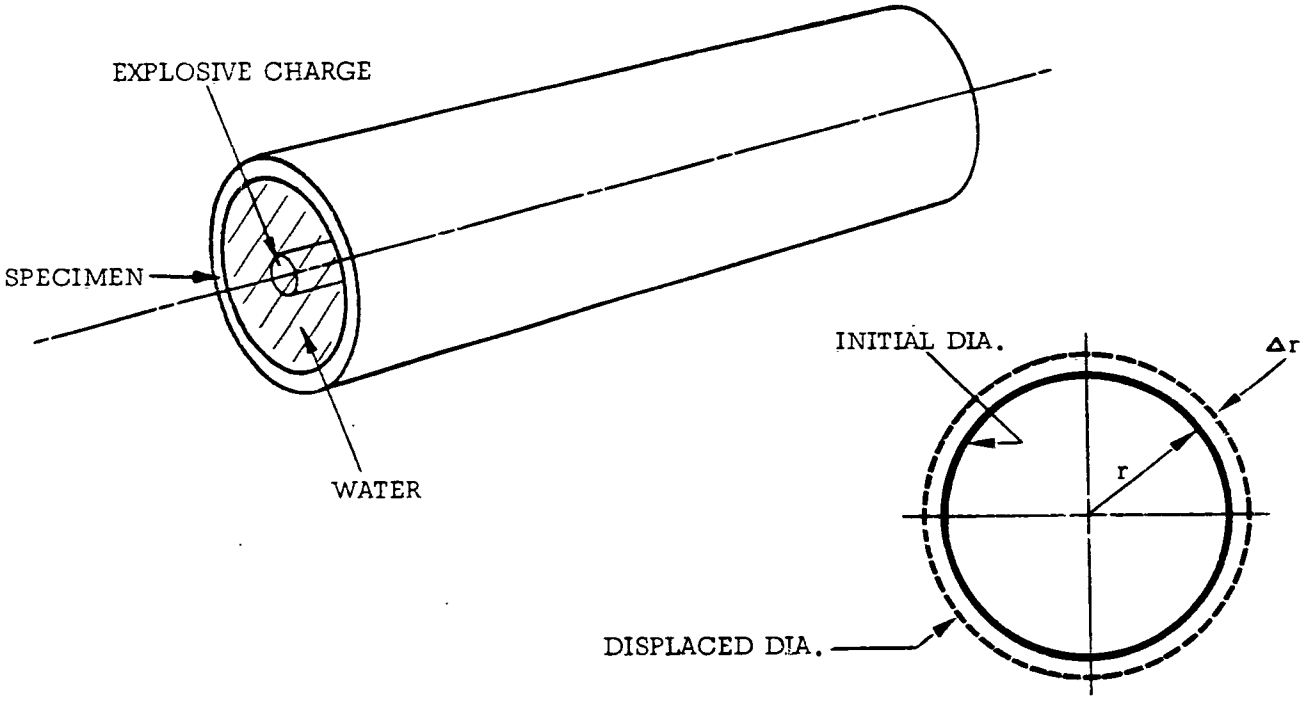

FIGURE 4.1 CHARGE CONFIGURATION FOR PRODUCING HIGH STRAIN RATES

Beckman & Whitley INC.
SAN CARLOS, CALIFORNIA

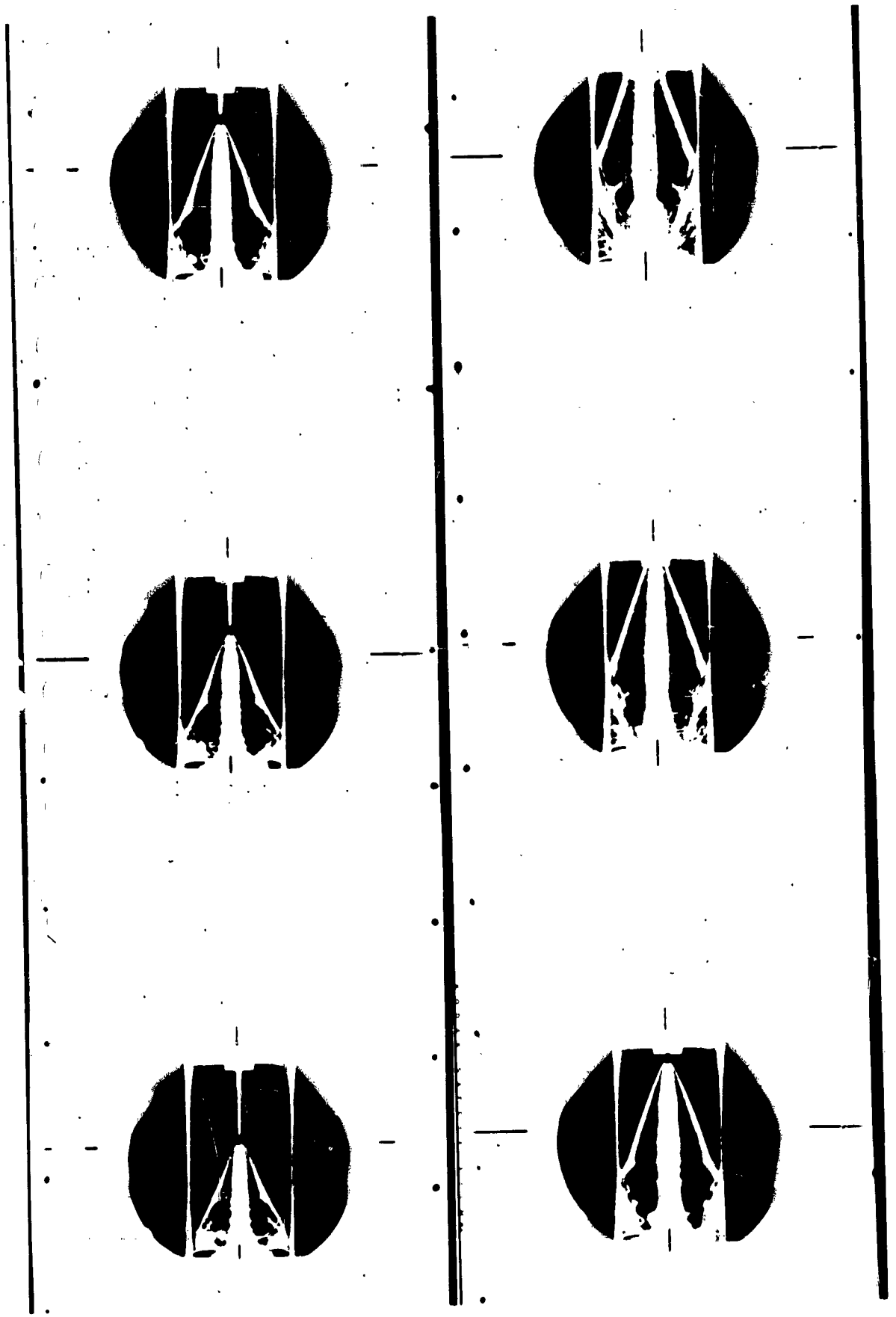

The test geometry and relevant quantities are shown in Fig. 4.1. The circumferential strain is given by

$$\epsilon = \frac{\Delta r}{r}$$

The stress strain curve is idealized as shown in Fig. 4.3(a). The energy balance, on a per unit volume basis, is given by

$$\frac{1}{2}\rho\,(v^2 - v_o^2) = \int_0^{\epsilon_1} E\epsilon d\epsilon + \int_0^{\epsilon} S_u d\epsilon \qquad (4.1)$$

$$= \frac{1}{2} E\epsilon_1^2 + S_u\,(\epsilon - \epsilon_1)$$

For the elastic regime this equation can be put in the form

$$\left(\frac{v}{v_o}\right)^2 = 1 - \frac{E}{\rho v_o^2}\left(\frac{\Delta r}{r}\right)^2 \qquad (4.2)$$

which indicates that the modulus of elasticity can be obtained from the slope of the curve shown in Fig. 4.3(b).

If the elastic energy is negligible, equation (4.1) may be written as

$$v_o^2 - v^2 = \frac{2S_u}{\rho r}\,\Delta r \qquad (4.3)$$

or

$$\frac{v^2}{v_o^2} = 1 - \frac{2S_u}{\rho v_o^2}\,\frac{\Delta r}{r} \qquad (4.4)$$

It is seen from this simple form that the graph of velocity squared against displacement should be

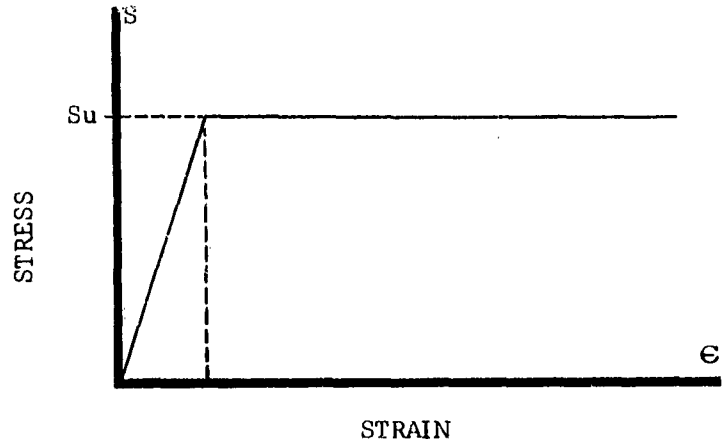

FIG. 4.3a IDEALIZED STRESS-STRAIN CURVE

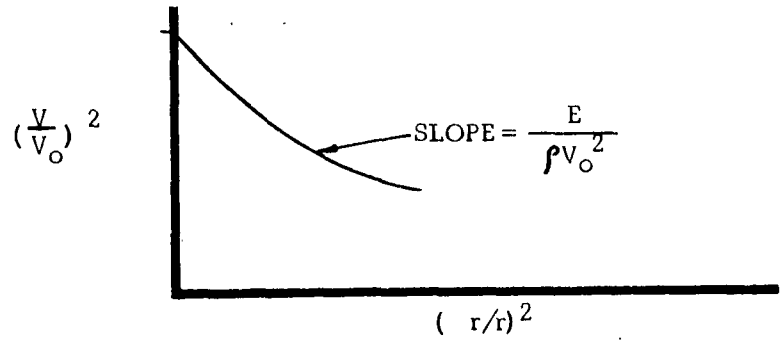

FIG. 4.3b PLOT FOR DETERMINING ELASTIC MODULUS

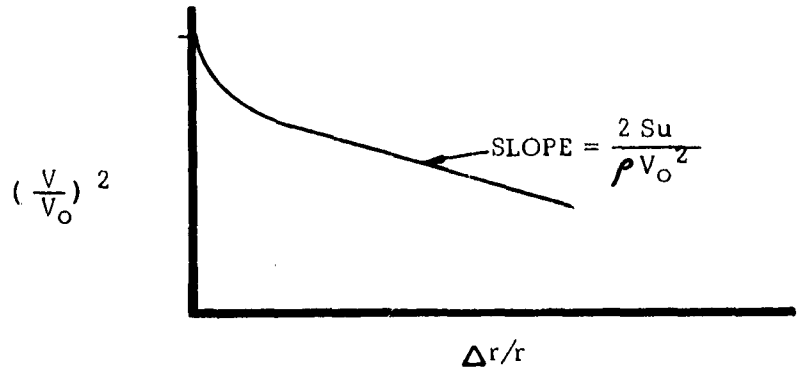

FIG. 4.3c PLOT FOR DETERMINING PLASTIC YIELD STRESS

linear as shown in Fig. 4.3(c), with the slope of the line giving the coefficient $\frac{2S_u}{\rho v_o^2}$ from which it is a simple matter to compute S_u.

The rate of strain involved is easily computed from

$$\frac{d\epsilon}{dt} = \frac{V}{r} \tag{4.5}$$

and thus may be varied by adjusting the specimen diameter and the initial velocity. This initial velocity may be estimated from the formula (12)

$$\frac{V}{D} = 0.38 \frac{\rho e}{\rho w} \left[\left(\frac{r_2}{r_1}\right)^2 - 1 \right]^{0.4} \tag{4.6}$$

where D is the detonation velocity of the explosive
ρw is the density of water
ρe is the density of explosive
r_1 is the radius of cylinder
r_2 is the radius of explosive

It is possible by adjustments of the charge geometry to vary the strain rate from 200/sec to 20,000/sec.

In this series of tests a Beckman & Whitley Model 189 Framing camera was used. The camera was focused on a region approximately one inch square which included the edge of the tube. Displacement of the tube wall was measured by a number of fine steel wires located at intervals of 0.125" between

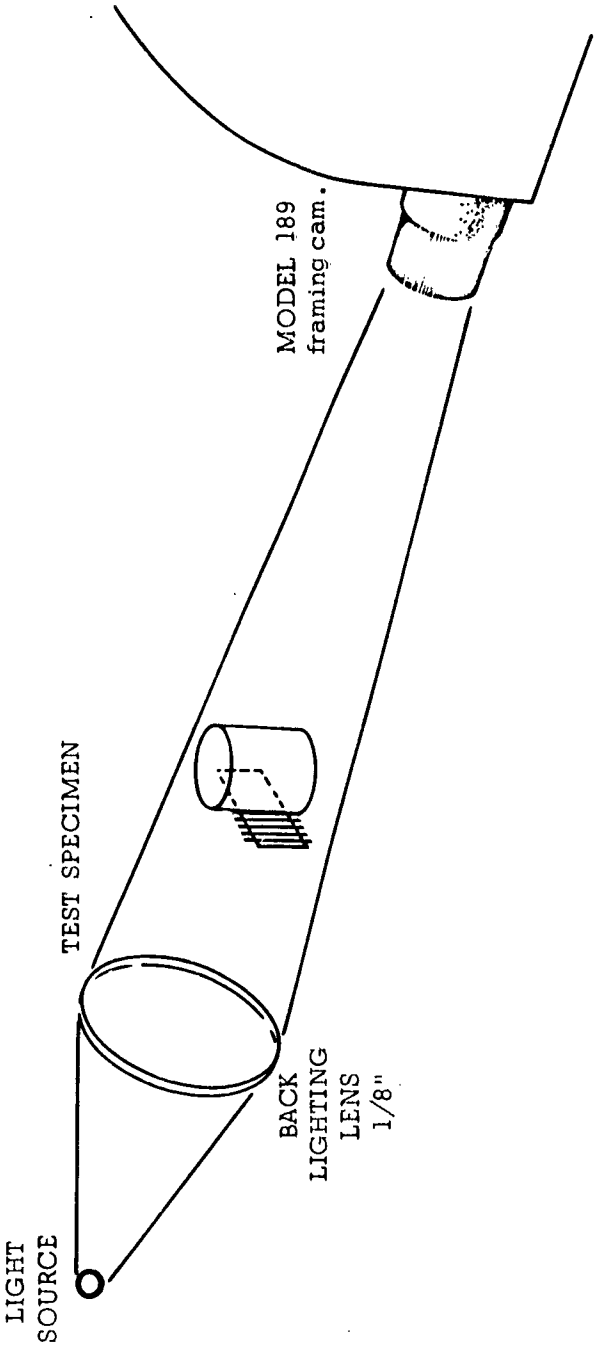

FIGURE 4.4 ARRANGEMENT OF TEST APPARATUS

machined guides. The arrangement is shown in Fig. 4.4.

Six tests were performed on tubes of 1", 2" and 3" diameter, at a number of mass ratios. A typical record, in this case of a 3" diameter tube, is shown in Fig. 4.5. Relevant date from the records is listed in Table V.

A typical data plot is given in Fig. 4.6. It can be seen from this graph that the V^2 vs $\frac{\Delta r}{r}$ curve is well approximated by a straight line over a large part of the time interval involved. This indicates that the idealization of the stress strain curve is justified in this range. A graph showing the variation of yield strength with strain rate is shown in Fig. 4.7.

The yield stresses observed at the lower strain rates, 31,000 lb/in^2, are lower than the minimum static yield stress given by the manufacturer (13), 42,000 lb/in^2. The probable cause of this difference is the anisotropy of the material. Such tubing is necessarily drawn in an axial direction, and when tested under longitudinal tension might be expected to exhibit a higher strength because of preferred grain orientation than when tested under a hoop stress, as in this experiment.

The results of this limited series of tests show that the method has considerable possibilities. It

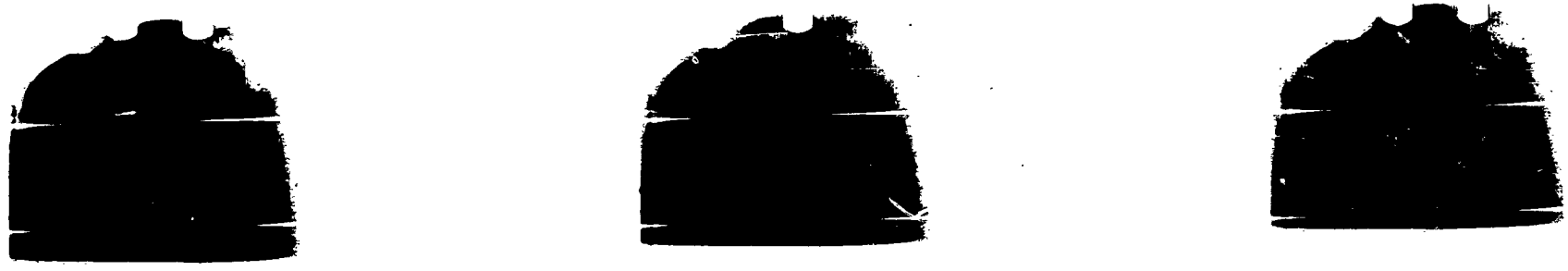

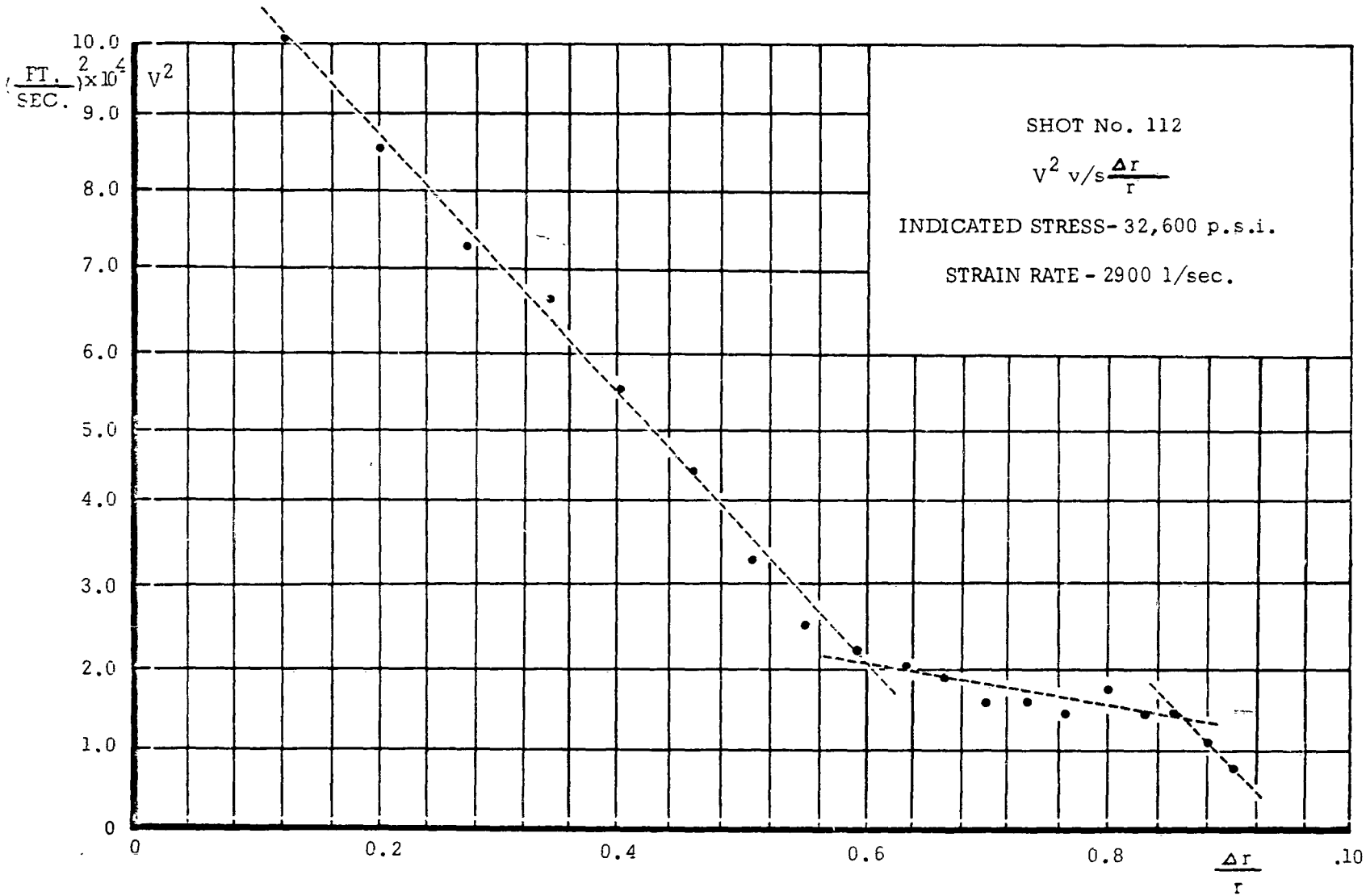

FIGURE 4.6 PLOT OF VELOCITY SQUARED v/s DISPLACEMENT FOR 2024 T4 ALUMINUM

Beckman & Whitley INC.
SAN CARLOS, CALIFORNIA

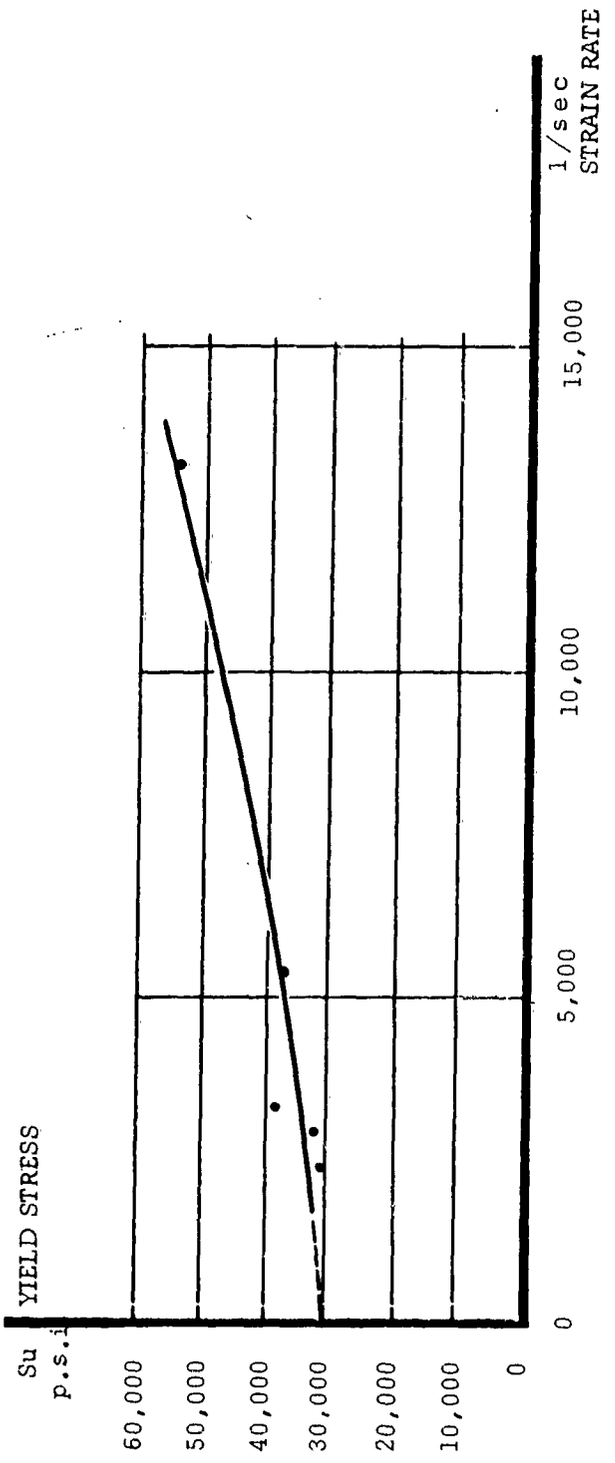

FIGURE 4.7 PLOT OF PLASTIC YIELD STRESS v/s STRAIN RATE FOR 2024 T4 ALUM.

TABLE V RESULTS OF YIELD STRENGTH TESTS

TEST No.	MASS RATIO	TUBE THICK.	APPARENT Y.S.p.s.i.	STRAIN RATE 1sec.
80	3"	3/32"	37,600	3,400
81	2"	2/32"		
82	1"	1/32"	54,000	13,200
83	3"	3/32"	31,000	2,400
111	3"	3/32"	38,500	3,240
112	2"	2/32"	32,600	2,900

Beckman & Whitley INC.
SAN CARLOS, CALIFORNIA

is simple in operation and in analysis. End effects are reduced to a minimum and the stress distribution during the test is essentially uniaxial. The values of the yield strength for 2024 T4 Al, are seen to be less than twice the static yield which is in accord with previous work.

V. CONCLUSIONS

1. Observations have been made of aluminum impacts using the technique of high speed photography. From the velocity measurements obtained, is has been possible to construct complete momentum and energy balances. The results indicate that the pressures and compressive stresses existing during impact may be estimated from standard shock theory. (More precise computations of these quantities are to be established by AMF on the basis of dislocation theory in a complementary contract.)

2. A few tests have been made on corrugated armor and the results indicate that this is a less efficient form of construction than solid armor. The results indicate that very thin foils may be treated as completely compressible material. Even less projectile deformation was observed with corrugated armor than with solid armor. Projectile fragmentation is not expected to be significant for velocities below 3000 ft/sec with aluminum projectiles.

3. A novel technique for observing the properties of materials at high strain rates characteristic of impacts has been developed. Results obtained on 2024 T4 aluminum indicate a factor of two in yield strength for an increase in strain rate from 10^3/sec to 10^4/sec.

BIBLIOGRAPHY

1. H. G. Hopkins and H. Kolsky, "The Mechanics of Hypervelocity Impact of Solids", Proc. 4th Hypervelocity Impact Symposium, Vol. I, paper 12, (1960)

2. S. C. Hunter, "Energy Absorbed by Elastic Waves during Impact", J.Mech.Phys.Solids, Vol. 5, p. 162, (1957)

3. N. Cristescu, "European Contributions to Dynamic Loading and Plastic Waves", Plasticity (2nd Symp. of Naval Struct. Mech.), Eds. E. H. Lee and P. S. Symonds, Pergamon Press, p. 385, (1961)

4. Goldsmith, "Impact", St. Martins Press, N. Y. Ch. t, (1960)

5. L. E. Fugelso, "Theoretical Study of Penetration and Residual Projectile Velocities", Personnel Armor Symposium, 4th, 5th Oct., 1961. U. S. Nav. Res. Lab., Washington, D. C.

6. M. H. Rice, R. G. McQueen and J. M. Walsh, "Compression of Solids by Strong Shock Waves", Solid State Physics, Vol. 6, 1-63, Academic Press, New York, (1958)

7. R. L. Bjork, "Numerical Solutions of the Axially Symmetric Hypervelocity Impact Process Involving Iron", Proc. 3rd Hypervelocity Impact Symposium, Vol. II, p. 35, (1958)

8. G. R. Fowles, "Shock Wave Compression of Hardened and Annealed 2024 Aluminum", J.App.Phys., Vol. 32, pp. 1475-1487, (1961)

9. A. E. Olshaker, "An Experimental Investigation in Lead of the Whipple 'Meteor Bumper'", Proc. 4th Hypervelocity Impact Symposium, Vol. II, paper 25, (1960)

10. M. J. Manjoine, "Influence of Strain Rate and Temperature on Yield Stress in Mild Steel", J.App.Mech., Vol. II, p. 211, (1944)

11. J. D. Campbell, "An Investigation of the Plastic Behavior of Metal Rods Subjected to Longitudinal Impact", J.Mech.Phys.Solids, Vol. I, pp. 113-123, (1953)

12. T. E. Holland, Final Report, George Washington University Research Laboratory, AD 306050, (1959)

13. Alcoa Structural Handbook, Aluminum Co. of America, Pittsburgh, Pennsylvania, (1960)